Abdominal Radiology (2019) 44:3166–3174
https://doi.org/10.1007/s00261-019-02107-y

PELVIS

Value of diffusion-weighted and dynamic contrast-enhanced MR in predicting parametrial invasion in cervical stromal ring focally disrupted stage IB–IIA cervical cancers

Jiacheng Song[1] · Qiming Hu[2] · Zhanlong Ma[1] · Jing Zhang[1] · Ting Chen[1]

Published online: 3 August 2019

Abstract

Objectives To compare the effectiveness of diffusion-weighted imaging (DWI) and dynamic contrast-enhanced (DCE) imaging in detecting parametrial invasion (PMI) in cervical stromal ring focally disrupted stage IB–IIA cervical cancers.

Methods Eighty-one patients with cervical stromal ring focally disrupted stage IB–IIA cervical cancers (PMI positive, $n=35$; PMI negative, $n=46$) who underwent preoperative MRI and radical hysterectomy were included in this study. Preoperative clinical variables and MRI variables were analyzed and compared.

Results The K_{trans} (min, mean, 10%, 25%, 50%, 75%, 90%), K_{ep} (min, 10%, 25%, 50%, 75%, 90%), and V_e (min, 10%, 25%, 50%, 75%, 90%) values of patients with PMI were significantly higher than patients without PMI. The apparent diffusion coefficient (ADC) value did not show statistical difference between the two groups (1.01 ± 0.21 vs. 0.97 ± 0.20 10^{-3} mm^2/s, $p=0.360$). Tumor craniocaudal planes were higher in PMI-positive group than PMI-negative group (35.84 ± 15.39 vs. 29.70 ± 11.78 mm, $p=0.048$). Tumor craniocaudal planes combined with $K_{ep\ min}$ value showed the highest area under the curve (AUCs) of 0.775, with a sensitivity of 72.7% and a specificity of 71.1% ($p=0.000$).

Conclusions DCE parameters combined tumor craniocaudal planes may represent a prognostic indicator for PMI in cervical stromal ring focally disrupted IB–IIA cervical cancers.

Keywords Cervical cancer · Dynamic contrast enhancement · Diffusion magnetic resonance imaging · Magnetic resonance imaging

Introduction

Parametrial invasion (PMI) is one of the most important factors in cervical cancer staging and treatment because it is associated with recurrence and poor prognosis [1]. High PMI risk cervical cancer patients were recommended surgery with removal of the parametrium or primary concurrent chemoradiation therapy [2, 3]. Low PMI risk cervical cancer patients were suggested less radical surgery [4, 5]. Parametrectomy was associated with increased morbidity and mortality related to postoperative complications such as fistula formation, ureteral injury, and bladder dysfunction [6–8]. Therefore, accurate assessment of PMI is important for treatment planning and prognosis.

Obvious PMI is easy to diagnose on MRI in higher stage cervical cancer patients. PMI exclusion is usually evaluated by a preserved hypointense stromal ring on T_2-weighted imaging (T_2WI) [9]. However, if the stromal ring is focally disrupted, it may be very difficult to determine PMI [10, 11]. Previous researches on MRI parameters in detecting PMI included all patients from stage IA2 to IIA, which included a part of early stage cervical cancers with definitely no PMI [12, 13]. Our research restricted the inclusion criteria to stromal ring focally disrupted cervical cancers which were very difficult to differentiate on conventional MRI but crucial to treatment planning.

✉ Jing Zhang
zhangjing_20180907@126.com

✉ Ting Chen
chentingwzc@163.com

[1] Department of Radiology, The First Affiliated Hospital of Nanjing Medical University, No. 300, Guangzhou Road, Nanjing 210029, China

[2] Department of Obstetrics & Gynecology, The First Affiliated Hospital of Nanjing Medical University, Nanjing 210029, China

Previous research papers concluded that the presence of PMI on MRI, tumor diffusion-weighted imaging (DWI), large tumor size, lymphovascular space invasion and deep stromal invasion were risk factors of PMI [14–17]. We focused on preoperative multiparametric MRI features rather than pathologic features for more meaningful differentiation and treatment guidance.

Dynamic contrast-enhanced (DCE) MRI parameters have been correlated with cervical cancer response to chemoradiotherapy and tumor recurrence [18, 19]. It assesses extravasation of paramagnetic contrast agents to reflect tumor microcirculation in vivo [20]. To our knowledge, DCE MRI in differentiating PMI in cervical cancers has not yet been well determined [21].

Therefore, the purpose of this study was to compare the effectiveness of DWI and DCE MRI in differentiating PMI in cervical stromal ring focally disrupted stage IB–IIA cervical cancers.

Materials and methods

Patients

This retrospective study was approved by our institutional review board and informed consent was waived. Between January 2011 and December 2017, 566 stage IB–IIA cervical cancer patients with preoperative MRI were screened. Of these, 103 patients showed cervical stromal ring focally disrupted on T_2WI. Exclusion criteria were as follows: (a) patients who received any chemoradiotherapy before MRI; (b) DCE and DWI sequence were not included in the MRI; (c) short time from conization or biopsy to MRI; (d) cystic mucinous adenocarcinoma pathological type; (e) no clinical and pathological reports in our hospital. Eighty-one patients treated with radical hysterectomy were finally included (Fig. 1). FIGO stage was evaluated by a gynecologist combining clinical examination with MRI.

Pathologic findings including the presence and absence of PMI, histologic type, pathology grade, lymphovascular space invasion, and lymph node metastasis were obtained from medical pathologic records.

MRI protocol

MR examinations were performed using a 3.0-Tesla MR scanner (MAGNETOM TrioTim, Siemens, Erlangen, Germany), with a 16-element pelvic phased-array coil. Single-shot echo-planar diffusion-module sequence parameters (repetition time ms/echo time ms, 6800/98; field of view, 250×250 mm^2; matrix, 192×130; section thickness, 3.0 mm). Diffusion was measured using b values of 0 and

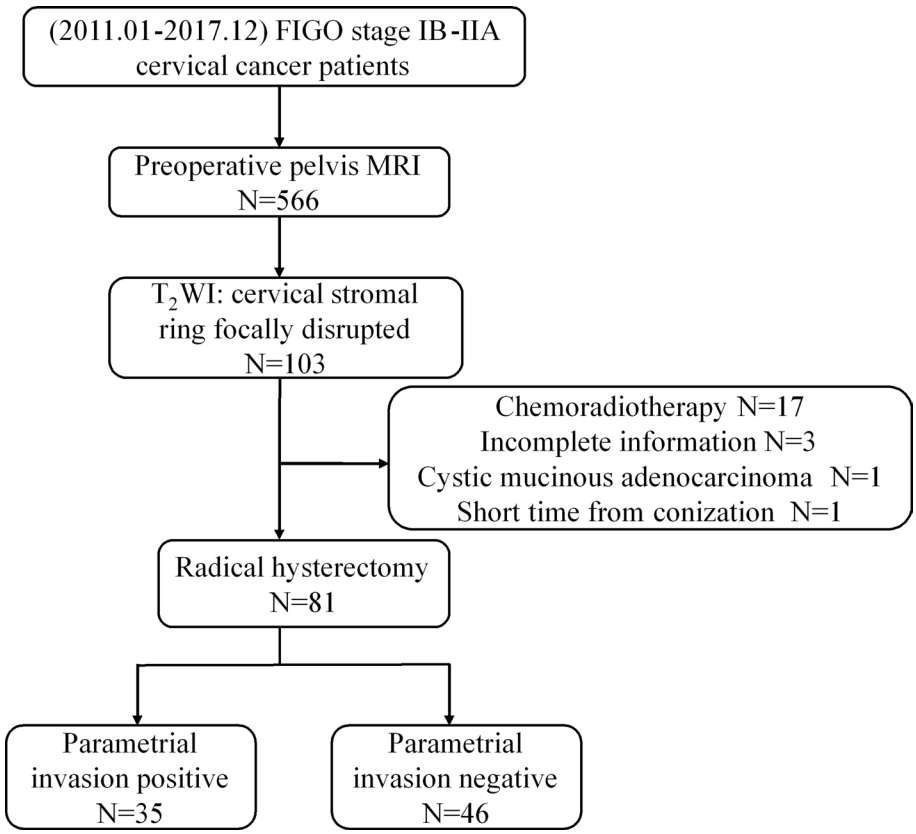

Fig. 1 Flow chart of the study design

800 s/mm^2, and ADC maps were automatically generated. DCE images sequence parameters (repetition time ms/echo time ms, 5.32/1.81; section thickness, 3.0 mm; intersection gap, 0.3 mm; field of view, 250 × 250 mm^2; matrix, 256 × 161, 10 sagittal slices, 25 periods, 4 min). An automated injector system (Stellant MR Injection System, Medrad, Germany) was used (GE HealthCare, 0.5 mmol/ml; dosage (ml) = weight (kg) × 0.2 ml/kg), with a flow rate of 3 ml/s.

Image analysis

Images were assessed by two experienced genitourinary radiologists with 8 and 5 years of experience in female pelvic MRI. The radiologists were blinded to the clinical information and pathologic results.

Suspected diagnosis of PMI was evaluated by the radiologists on conventional MRI. Cervical stromal ring focally disrupted was evaluated as the discontinuity of the dark ring on T_2WI.

Tumor size (transverse) was defined as the horizontal diameter on axial images and tumor size (anteroposterior) was defined as the vertical diameter on axial images. Tumor size (craniocaudal planes) was defined as the tumor diameter parallel to the uterus on sagittal images.

For ADC value measurement, all DWI data were converted into DICOM format and processed with software (FireVoxel; CAI^{2}R; New York University, NY). The mean ADC value was calculated using the following exponential fitting formula: $\mathrm{ADC} = -\ln(S_b/S_0)/b$, where b represents the diffusion sensitivity coefficients, and S_b and S_0 represent the corresponding signal values of the given region of interest (ROI). The ROI was measured at the center of the tumors.

For measurement of DCE-MR parameters, we carried out a pharmacokinetic analysis using non-commercial software (Omnikinetics, GE Healthcare, Shanghai, China). A fully automated, image-based, individualized arterial input function (AIF) estimation method was used. The parameters—including the volume transfer constant between blood plasma and extracellular-extravascular space (EES) (K_{trans}, min^{-1}), rate constant between EES and blood plasma (K_{ep}, min^{-1}), and volume of EES space per unit volume of tissue (V_e)—were derived from the entire ROIs for each patient. The radiologists manually drew ROIs covering the whole tumors. Then histogram features of the tumor perfusion parameters including min, max, mean, 10%, 25%, 50%, 75%, 90% were calculated.

Mean ADC value and DCE-MR parameters were assessed by two experienced genitourinary radiologists and the averaged results were used.

Statistical analysis

Statistical analysis was performed using PASW statistical software (18.0 SPSS Inc, Chicago, IL, USA; MedCalc, version 11.5, Mariakerke, Belgium). The Student t test was used to compare age, tumor size, ADC value, and DCE parameters between PMI-positive and PMI-negative groups. Pearson's Chi-square test was used to compare FIGO stage, histologic type, pathology grade, lymphovascular space invasion, lymph node metastasis, and suspected diagnosis of PMI. To evaluate the diagnostic performance of tumor size, K_{trans}, K_{ep}, and V_e in differentiating PMI, receiver-operating-characteristic (ROC) analysis was performed. Therefore, we also calculated the area under the curve (AUC), sensitivity, and specificity. To test the reproducibility of ADC value and DCE parameters, intra-class correlation coefficient (ICC) values were calculated with a 95% confidence interval (CI). A statistically significant difference was denoted when the p value was less than 0.05.

Results

Patients

In the current study, we enrolled 81 cervical stromal ring focally disrupted cervical cancer patients (35 patients with positive PMI and 46 patients with negative PMI). PMI rate was 43.2% in cervical stromal ring focally disrupted cervical cancers. The average age and pathology grade were not statistically significant between the two groups. Higher FIGO stage patients account more in PMI-positive group ($p = 0.033$). Lymphovascular space invasion and lymph node metastases account more in PMI-positive group ($p = 0.034$ and 0.023, respectively) (Table 1).

Conventional MR

Tumor craniocaudal planes were superior to transverse and anteroposterior diameters in predicting PMI. Tumor craniocaudal planes were larger in PMI-positive group compared with negative group ($p = 0.048$). Suspected diagnosis of PMI from conventional MR did not show statistical difference (Table 2).

DWI and DCE parameters

Tumor mean ADC value did not show statistical difference between PMI-positive and PMI-negative groups ($p = 0.360$).

A comparison of the DCE parameters according to clinicopathological features is shown in Table 2. Higher K_{trans} (min, mean, 10%, 25%, 50%, 75%, 90%), K_{ep} (min, 10%, 25%, 50%, 75%, 90%), and V_e (min, 10%, 25%, 50%, 75%,

Table 1 Patients' clinicopathological characteristics

Variables	PMI (+) ($n=35$)	PMI (−) ($n=46$)	p value
Age (years)	49.43 ± 9.88	52.09 ± 9.54	0.228
FIGO stage [n (%)]			0.033*
IB1	9 (25.7)	24 (52.2)	
IB2	6 (17.1)	6 (13.0)	
IIA	20 (57.1)	16 (34.8)	
Histologic type [n (%)]			
SCC	27 (77.1)	37 (80.4)	0.787
Non-SCC	8 (22.9)	9 (19.6)	
Pathology grade > II [n (%)]	18 (51.43)	29 (63.04)	0.435
Lymphovascular space invasion [n (%)]	29 (82.86)	26 (56.52)	0.034*
Lymph node metastasis [n (%)]	18 (51.43)	12 (26.09)	0.023*

PMI parametrial invasion, *FIGO* International Federation of Gynecology and Obstetrics, *SCC* squamous cell carcinoma

*$p < 0.05$

Table 2 Comparison of MRI variables between patients with and without PMI

Variables	PMI (+) ($n=35$)	PMI (−) ($n=46$)	p value
Tumor size (transverse) (mm)	34.08 ± 10.30	30.92 ± 10.88	0.189
Tumor size (anteroposterior) (mm)	29.15 ± 11.14	28.09 ± 10.74	0.667
Tumor size (CC) (mm)	35.84 ± 15.39	29.70 ± 11.78	0.048*
Tumor ADC value (10^{-3} mm^2/s)	1.01 ± 0.21	0.97 ± 0.20	0.360
Suspected diagnosis of PMI [n (%)]	16 (45.71)	13 (28.26)	0.181
$K_{\text{trans min}}$ (min^{-1})	0.26 ± 0.18	0.12 ± 0.18	0.002*
$K_{\text{trans max}}$ (min^{-1})	2.67 ± 1.59	2.11 ± 1.24	0.086
$K_{\text{trans mean}}$ (min^{-1})	0.92 ± 0.42	0.62 ± 0.30	0.000*
K_{trans} 10% (min^{-1})	0.51 ± 0.24	0.29 ± 0.24	0.000*
K_{trans} 25% (min^{-1})	0.64 ± 0.28	0.39 ± 0.26	0.000*
K_{trans} 50% (min^{-1})	0.86 ± 0.40	0.55 ± 0.31	0.000*
K_{trans} 75% (min^{-1})	1.12 ± 0.55	0.76 ± 0.38	0.002*
K_{trans} 90% (min^{-1})	1.42 ± 0.74	1.02 ± 0.54	0.011*
$K_{\text{ep min}}$ (min^{-1})	0.52 ± 0.40	0.26 ± 0.37	0.004*
$K_{\text{ep max}}$ (min^{-1})	4.49 ± 2.13	4.18 ± 1.79	0.477
$K_{\text{ep mean}}$ (min^{-1})	1.89 ± 0.74	1.61 ± 0.76	0.115
K_{ep} 10% (min^{-1})	1.09 ± 0.45	0.78 ± 0.50	0.007*
K_{ep} 25% (min^{-1})	1.35 ± 0.55	1.06 ± 0.60	0.031*
K_{ep} 50% (min^{-1})	1.79 ± 0.66	1.42 ± 0.73	0.024*
K_{ep} 75% (min^{-1})	2.30 ± 0.92	1.82 ± 0.88	0.022*
K_{ep} 90% (min^{-1})	2.81 ± 1.27	2.26 ± 0.97	0.033*
$V_{\text{e min}}$	0.22 ± 0.16	0.11 ± 0.15	0.003*
$V_{\text{e max}}$	0.86 ± 0.18	1.06 ± 0.87	0.187
$V_{\text{e mean}}$	0.51 ± 0.18	0.42 ± 0.20	0.063
V_{e} 10%	0.37 ± 0.15	0.24 ± 0.16	0.001*
V_{e} 25%	0.42 ± 0.17	0.29 ± 0.16	0.001*
V_{e} 50%	0.49 ± 0.17	0.36 ± 0.17	0.002*
V_{e} 75%	0.57 ± 0.17	0.45 ± 0.17	0.004*
V_{e} 90%	0.65 ± 0.17	0.55 ± 0.17	0.016*

K_{trans} volume transfer constant between extravascular-extracellular space and blood plasma (min^{-1}), K_{ep} rate constant from extravascular-extracellular space to blood plasma (min^{-1}), V_{e} extravascular-extracellular space volume per unit tissue volume

PMI parametrial invasion, *CC* craniocaudal planes, *ADC* apparent diffusion

*$p < 0.05$

90%) values were noted in PMI-positive than PMI-negative cervical cancers. Figures 2 and 3 illustrate the comparison of $K_{trans\ mean}$ between the two groups.

The ROC analysis was used to find the reasonable threshold of perfusion parameters and tumor craniocaudal planes to differentiate PMI from cervical stromal ring focally disrupted cervical cancers (Table 3). The $K_{trans\ 10\%}$ showed the highest AUCs of 0.774 ($p = 0.000$), with a cutoff value of 0.34, sensitivity of 87.9%, and specificity of 67.4%, respectively.

Tumor craniocaudal planes combined with $K_{ep\ min}$ showed the highest AUCs of 0.775 ($p = 0.000$), with a sensitivity of 72.7% and a specificity of 71.1%, respectively (Table 3; Fig. 4).

In the evaluation of inter-observer agreement (ICC) for the ADC and DCE parameters, ICC values showed a good level of agreement: 0.848 (95% CI 0.763–0.903) for ADC, 0.917 (95% CI 0.870–0.974) for $K_{trans\ mean}$, 0.889 (95% CI 0.827–0.929) for $K_{ep\ mean}$, and 0.857 (95% CI 0.776–0.908) for $V_{e\ mean}$.

Discussion

In this study, we evaluated the usefulness of DWI and perfusion parameters derived from DCE for assessing PMI in cervical stromal ring focally disrupted cervical cancers. Our results showed that PMI-positive cervical cancers had higher perfusion parameters. However, DWI did not show a good identification ability. Tumor craniocaudal planes together with $K_{ep\ min}$ can help improve the diagnostic ability with AUCs of 0.775.

As described in previous reports, positive predictive value of disruption of the cervical stromal ring on MRI for PMI was quite low (around 60%) [22]. In another comparison study, the sensitivity of conventional MRI in detecting PMI is 44.4% [23]. Our research showed the PMI rate to be about 43.2% in cervical stromal ring focally disrupted cervical cancers. We deduced that conventional MRI had a low sensitivity in detecting PMI and pathologic PMI rate was low in stromal ring focally disrupted cervical cancers.

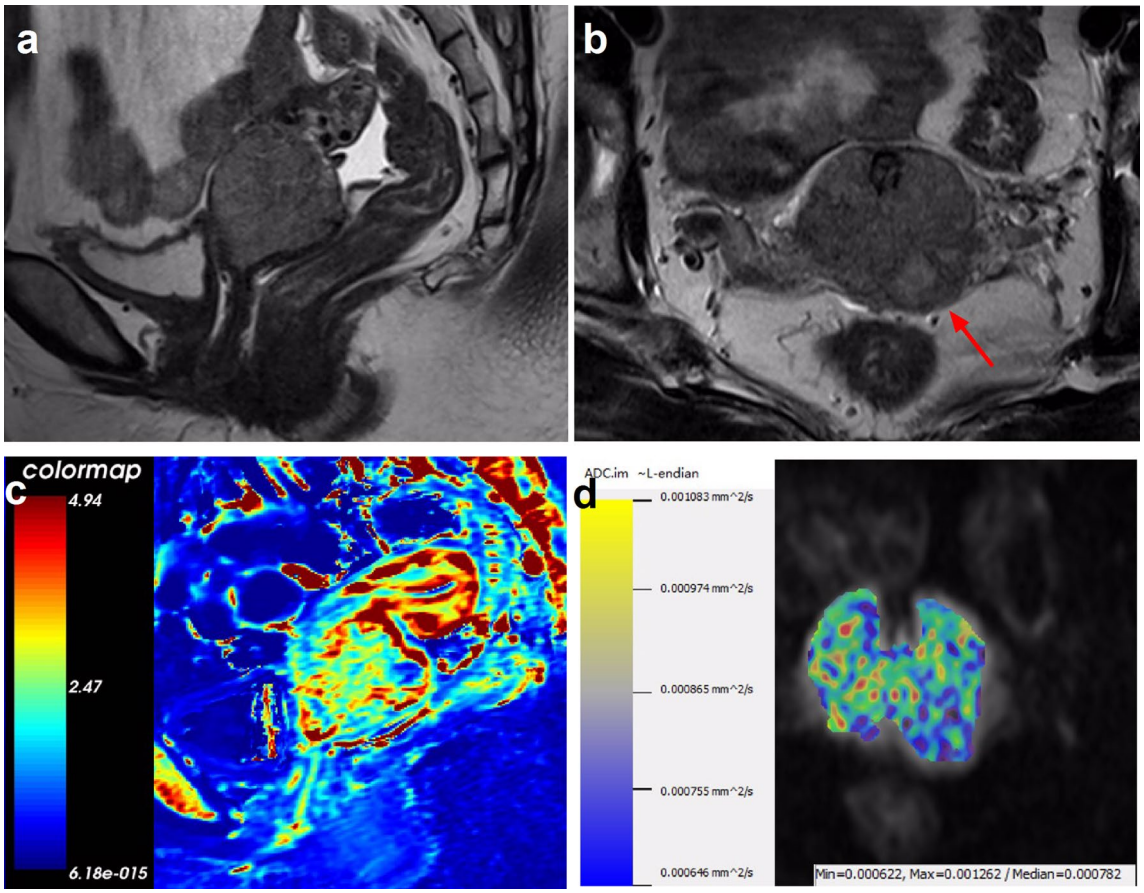

Fig. 2 A 55-year-old woman with cervical stromal ring focally disrupted cervical cancer, which was confirmed pathologically to be PMI negative. **a** Sagittal T_2-weighted image demonstrates a hyperintense cervical mass. **b** Disruption of cervical stromal ring on the left back side (arrow). **c** $K_{trans\ mean}$ parameter was relatively low in the tumor (0.25 min^{-1}). **d** The ADC value of the lesion was 0.874×10^{-3} mm^2/s

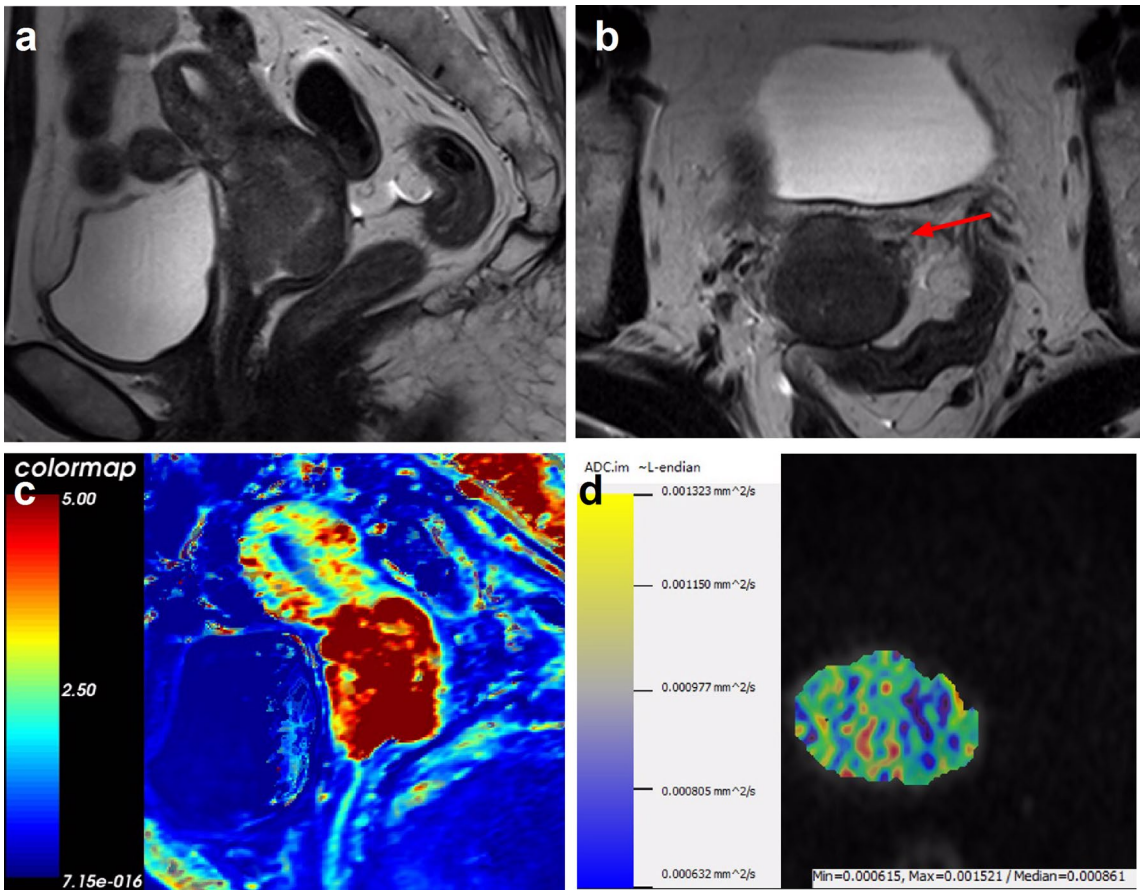

Fig. 3 A 61-year-old woman with cervical stromal ring focally disrupted cervical cancer, which was confirmed pathologically to be PMI positive. **a** Sagittal T2-weighted image demonstrates a hyperintense cervical mass. **b** Disruption of cervical stromal ring on the left anterior side (arrow). **c** $K_{trans\ mean}$ parameter was relatively high in the tumor (0.78 min^{-1}). **d** The ADC value of the lesion was 0.959×10^{-3} mm^2/s

Regarding the previous investigations related with PMI in cervical cancers, DWI seems to be a robust and valuable marker, especially when fused with T_2WI [11, 13, 21]. Park et al. [12] concluded that tumor ADC value was an independent predictor for PMI. Woo et al. [24] revealed that ADC values and T_2WI-based Likert score for radiological PMI were significantly associated with PMI. However, our findings showed the opposite result. ADC values in cervical stromal ring focally disrupted cervical cancers cannot differentiate PMI. We deduced that the most important reason may due to the different inclusion criteria. Most of the tumors in our research were relatively large and had higher pathological grade. This group of patients can be classified to have a score of 3 (possible) in a research by Woo et al. [24]. The ADC value cannot differentiate PMI with interscore 3 ($p = 0.857$), the result of which were same as that of our research. Therefore, ADC value may be insufficient to distinguish PMI in cervical stromal ring focally disrupted cervical cancers.

Larger maximum clinical tumor sizes (> 3 cm) were reported to be an independent risk factor for PMI in stage IB–IIA cervical cancer [1, 16]. Moreover, a cutoff value of 3 cm in clinical tumor size was also referred as an independent prognostic factor for a 3-year disease-free interval [25]. Hayashi et al. [26] revealed tumor craniocaudal planes to be the most critical factor in predicting prognosis in cervical cancers, and one of our previous research also showed that tumor craniocaudal plane was more sensitive in detecting lymph node metastasis in cervical cancers. In our study, a significant correlation was also found between tumor craniocaudal planes and PMI with a cutoff value of 2.5 cm.

DCE parameters have been related to cervical cancer chemoradiotherapeutic response [27], differentiation of benign and malignant cervical lesions [28], pathologic angiogenic activity [29], and evaluation of tumor vasculature and vascular permeability [30]. None of the previous researches focused on the relationship of DCE parameters

Table 3 Effectiveness in predicting PMI in cervical stromal ring focally disrupted cervical cancers

Variables	Cut-off value	AUC	95% CI	Sensitivity (%)	Specificity (%)	*p* value*
K_{trans} 10% (min^{-1})	> 0.34	0.774	0.669–0.879	87.9	67.4	0.000
K_{trans} 25% (min^{-1})	> 0.42	0.757	0.650–0.864	84.8	63.0	0.000
K_{trans} 50% (min^{-1})	> 0.48	0.734	0.626–0.842	93.9	52.2	0.000
$K_{trans\ mean}$ (min^{-1})	> 0.54	0.715	0.603–0.827	93.9	45.7	0.001
K_{trans} 90% (min^{-1})	> 0.70	0.659	0.538–0.781	93.9	37.0	0.016
$K_{ep\ min}$ (min^{-1})	> 0.64	0.720	0.603–0.836	48.5	89.4	0.001
K_{ep} 10% (min^{-1})	> 0.88	0.688	0.570–0.806	72.7	61.7	0.004
K_{ep} 75% (min^{-1})	> 1.98	0.666	0.545–0.787	66.7	66.0	0.012
V_e 10%	> 0.28	0.741	0.632–0.851	78.8	68.1	0.000
V_e 25%	> 0.34	0.736	0.625–0.846	72.7	70.2	0.000
$V_{e\ min}$	> 0.12	0.725	0.612–0.839	72.7	68.1	0.001
V_e 50%	> 0.42	0.725	0.614–0.835	60.6	76.6	0.001
Tumor CC (mm)	> 24.75	0.637	0.515–0.759	91.2	37.8	0.038
Tumor (CC) combine K_{ep} min		0.775	0.673–0.877	72.7	71.1	0.000
Tumor (CC) combine K_{trans} 10%		0.768	0.664–0.872	48.5	91.1	0.000
Tumor (CC) combine V_e 10%		0.746	0.637–0.855	66.7	75.6	0.000

CC craniocaudal planes, *AUC* area under the curve, *CI* confidence interval

*$p < 0.05$

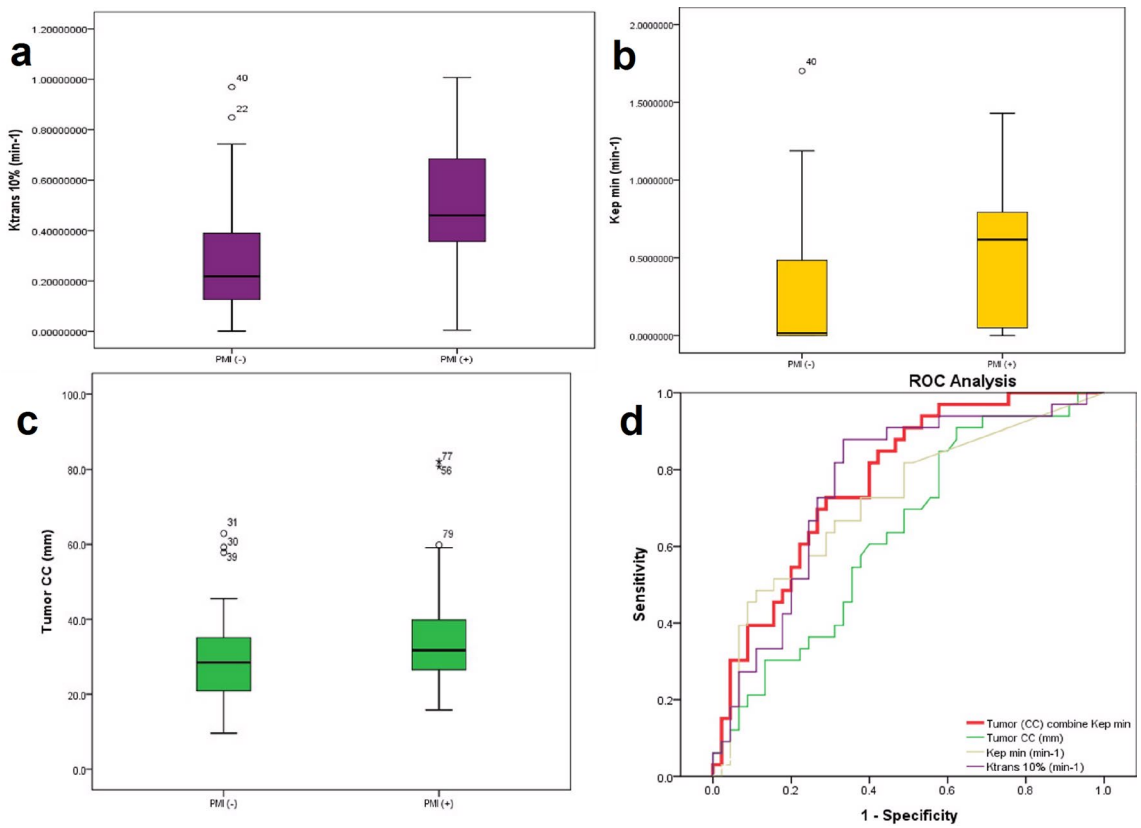

Fig. 4 Box plots showing K_{trans} 10%, $K_{ep\ min}$ and tumor craniocaudal planes in cervical cancers with and without PMI. K_{trans} 10% (**a**), $K_{ep\ min}$ (**b**), and tumor craniocaudal planes (**c**) were significantly higher in the cervical cancers with positive PMI. **d** ROC analysis of K_{trans} 10% (purple), $K_{ep\ min}$ (yellow), tumor craniocaudal planes (green), and the combination of $K_{ep\ min}$ and tumor craniocaudal planes (red) (AUC = 0.775)

with PMI. More aggressive tumors commonly exhibit a more rapid and obvious enhancement and washout, which may represent a higher vascular density, permeability, and greater interstitial space [31]. Loss of function of cell–cell adhesion molecules, such as e-cadherin, is a crucial step in tumor region progression [32, 33], such as regional PMI in our research. PMI-positive tumors with larger interstitial space can be reflected by higher DCE parameters. Higher perfusion parameters especially K_{trans} of 10% in our study imply that perfusion parameters may serve as an effective indicator in the differentiation of PMI.

The results of this study also indicate that lower percentage of K_{trans}, K_{ep}, and V_e all showed higher diagnostic ability in differentiating PMI-positive cervical cancers. Combining tumor craniocaudal planes and perfusion parameters especially $K_{ep\ min}$ can achieve the highest AUC value of 0.775, with a sensitivity of 72.7% and a specificity of 71.1%. According to the previous research, conventional MR had a sensitivity of 38% and a specificity of 99% in the diagnosis of PMI [34]. The high specificity rate may be because of the inclusion criteria and the preserved stromal ring can be easily identified on T_2WI. However, in our research, MR had a relatively low specificity rate in detecting stromal ring focally disrupted cervical cancers. Another study found tumor volume showed a sensitivity of 59.26% and a specificity of 61.54% in detecting PMI [35]. We combined tumor volume with perfusion parameters, which can increase both the sensitivity and specificity.

There are several limitations of this study. First, low signal intensity cervical stromal ring was not obvious in some cervical cancer patients. The evaluation was a bit more difficult in this group of patients. Second, higher DCE parameters were explained as hypervascularity, high permeability, and leakiness. This hypothesis has not been pathologically confirmed. Therefore, immunohistochemical staining (such as microvessel density, vascular endothelial growth factor, CD31, extracellular matrix protein) of the surgical specimens is further required. Third, only mean ADC value was compared in our research. Histogram analysis, texture analysis, diffusion kurtosis imaging (DKI), or intravoxel incoherent motion (IVIM) need to be further compared. Fourth, some prognostic factors such as 5-year survival rate or distant metastasis rate can be further researched between the two groups.

In conclusion, DCE parameters and tumor craniocaudal planes may represent a prognostic indicator of PMI in cervical stromal ring focally disrupted cervical cancers. We propose that the combined use of DCE and tumor craniocaudal planes can aid in accurate evaluation of PMI and surgical planning and risk stratification.

Compliance with ethical standards

Conflict of interest The authors declare that they have no conflict of interest.

References

1. E. Canaz, E.S. Ozyurek, B. Erdem, M. Aldikactioglu Talmac, I. Yildiz Ozaydin, O. Akbayir, C. Numanoglu, V. Ulker (2017), Preoperatively Assessable Clinical and Pathological Risk Factors for Parametrial Involvement in Surgically Treated FIGO Stage IB-IIA Cervical Cancer, Int. J. Gynecol. Cancer. 27: 1722–1728.
2. D.C. Jung, M.K. Kim, S. Kang, S.S. Seo, J.Y. Cho, N.H. Park, Y.S. Song, S.Y. Park, S.B. Kang, J.W. Kim (2010) Identification of a patient group at low risk for parametrial invasion in early-stage cervical cancer, Gynecol. Oncol. 119: 426–430.
3. T.W. Kong, J.D. Lee, J.H. Son, J. Paek, M. Chun, S.J. Chang, H.S. Ryu (2016) Corrigendum to "Treatment outcomes in patients with FIGO stage IB–IIA cervical cancer and a focally disrupted cervical stromal ring on magnetic resonance imaging: A propensity score matching study" Gynecol. Oncol. 143: 77–82.
4. J. Kodama, T. Kusumoto, K. Nakamura, N. Seki, A. Hongo, Y. Hiramatsu (2011) Factors associated with parametrial involvement in stage IB1 cervical cancer and identification of patients suitable for less radical surgery, Gynecol. Oncol. 122: 491–494.
5. M.K. Kim, J.W. Kim, M.A. Kim, H.S. Kim, H.H. Chung, N.H. Park, I.A. Park, Y.S. Song, S.B. Kang (2010) Feasibility of less radical surgery for superficially invasive carcinoma of the cervix, Gynecol. Oncol. 119: 187–191.
6. F. Raspagliesi, A. Ditto, R. Fontanelli, F. Zanaboni, E. Solima, G. Spatti, F. Hanozet, F. Vecchione, G. Rossi, S. Kusamura (2006) Type II versus Type III Nerve-sparing Radical hysterectomy: Comparison of lower urinary tract dysfunctions, Gynecol. Oncol. 102: 256–262.
7. F. Aoun, R. van Velthoven (2015) Lower urinary tract dysfunction after nerve-sparing radical hysterectomy, Int. Urogynecol. J. 26: 947–957.
8. R.M. Laterza, K.-D. Sievert, D. de Ridder, M.E. Vierhout, F. Haab, L. Cardozo, P. van Kerrebroeck, F. Cruz, C. Kelleher, C. Chapple, M. Espuña-Pons, H. Koelbl (2015) Bladder function after radical hysterectomy for cervical cancer., Neurourol. Urodyn. 34: 309-315.
9. S.H. Kim, B.I. Choi, H.P. Lee, S.B. Kang, Y.M. Choi, M.C. Han, C.W. Kim (1990) Uterine cervical carcinoma: comparison of CT and MR findings., Radiology. 175: 45–51.
10. S.H. Kim, B.I. Choi, J.K. Han, H.D. Kim, H.P. Lee, S.B. Kang, J.Y. Lee, M.C. Han (1993) Preoperative staging of uterine cervical carcinoma: comparison of CT and MRI in 99 patients., J. Comput. Assist. Tomogr. 17: 633–640.
11. J.J. Park, C.K. Kim, S.Y. Park, B.K. Park (2015) Parametrial Invasion in Cervical Cancer: Fused T2-weighted Imaging and High- b -Value Diffusion-weighted Imaging with Background Body Signal Suppression at 3 T, Radiology. 274: 734–741.
12. J.J. Park, C.K. Kim, S.Y. Park, B.K. Park, B. Kim (2014) Value of diffusion-weighted imaging in predicting parametrial invasion in stage IA2-IIA cervical cancer, Eur. Radiol. 24: 1081–1088.
13. J.R. Qu, L. Qin, X. Li, J.P. Luo, J. Li, H.K. Zhang, L. Wang, N.N. Shao, S.N. Zhang, Y. Le Li, C.C. Liu, H.L. Li (2018) Predicting parametrial invasion in cervical carcinoma (stages IB1, IB2, and IIA): Diagnostic accuracy of T2-weighted imaging combined with DWI at 3 T, Am. J. Roentgenol. 210: 677–684.
14. M. Kim, D.H. Suh, K. Kim, H.J. Lee, Y.B. Kim, J.H. No (2017) Magnetic Resonance Imaging as a Valuable Tool for Predicting

Parametrial Invasion in Stage IB1 to IIA2 Cervical Cancer, Int. J. Gynecol. Cancer. 27: 332–338.
15. O. Gemer, R. Eitan, M. Gdalevich, A. Mamanov, B. Piura, A. Rabinovich, H. Levavi, B. Saar-Ryss, R. Halperin, S. Finci, U. Beller, I. Bruchim, T. Levy, I. Ben Shachar, A. Ben Arie, O. Lavie (2013) Can parametrectomy be avoided in early cervical cancer? An algorithm for the identification of patients at low risk for parametrial involvement., Eur. J. Surg. Oncol. 39: 76–80.
16. S.J. Chang, R.E. Bristow, H.S. Ryu (2012) A model for prediction of parametrial involvement and feasibility of less radical resection of parametrium in patients with FIGO stage IB1 cervical cancer, Gynecol. Oncol. 126: 82–86.
17. J. Scheidler, A.F. Heuck, M. Steinborn, R. Kimmig, M.F. Reiser (1998) Parametrial invasion in cervical carcinoma: evaluation of detection at MR imaging with fat suppression., Radiology. 206: 125–129.
18. J.J. Park, C.K. Kim, S.Y. Park, A.W. Simonetti, E.J. Kim, B.K. Park, S.J. Huh (2014) Assessment of early response to concurrent chemoradiotherapy in cervical cancer: Value of diffusion-weighted and dynamic contrast-enhanced MR imaging, Magn. Reson. Imaging. 32: 993–1000.
19. A. Jalaguier-Coudray, R. Villard-Mahjoub, A. Delouche, B. Delarbre, E. Lambaudie, G. Houvenaeghel, M. Minsat, A. Tallet, R. Sabatier, I. Thomassin-Naggara (2017) Value of Dynamic Contrast-enhanced and Diffusion-weighted MR Imaging in the Detection of Pathologic Complete Response in Cervical Cancer after Neoadjuvant Therapy: A Retrospective Observational Study, Radiology. 284: 432–442.
20. A.R. Padhani (2002) Dynamic contrast-enhanced MRI in clinical oncology: Current status and future directions, J. Magn. Reson. Imaging. 16: 407–422.
21. S. Woo, C.H. Suh, S.Y. Kim, J.Y. Cho, S.H. Kim (2018) Magnetic resonance imaging for detection of parametrial invasion in cervical cancer: An updated systematic review and meta-analysis of the literature between 2012 and 2016, Eur. Radiol. 28: 530–541.
22. KongT.W. Kong, J. Kim, J.H. Son, S.W. Kang, J. Paek, M. Chun, S.J. Chang, H.S. Ryu (2016) Preoperative nomogram for prediction of microscopic parametrial infiltration in patients with FIGO stage IB cervical cancer treated with radical hysterectomy, Gynecol. Oncol. 142: 109–114.
23. H.H. Chung, S.B. Kang, J.Y. Cho, J.W. Kim, N.H. Park, Y.S. Song, S.H. Kim, H.P. Lee (2007) Can preoperative MRI accurately evaluate nodal and parametrial invasion in early stage cervical cancer?, Jpn. J. Clin. Oncol. 37: 370–375.
24. S. Woo, S.Y. Kim, J.Y. Cho, S.H. Kim (2018) Apparent diffusion coefficient for prediction of parametrial invasion in cervical cancer: a critical evaluation based on stratification to a Likert scale using T2-weighted imaging, Radiol. Medica. 123: 209–216.
25. G. Delgado, B. Bundy, R. Zaino, B.U. Sevin, W.T. Creasman, F. Major (1990) Prospective surgical-pathological study of disease-free interval in patients with stage IB squamous cell carcinoma of the cervix: A Gynecologic Oncology Group study, Gynecol. Oncol. 38: 352–357.
26. T. Hayashi, T. Kato (1999) Usefulness of tumor size on MR imaging in assessing the prognosis of uterine cervical cancer treated with radiation. Nihon Igaku Hoshasen Gakkai Zasshi. 59: 250–255.
27. E.K.F. Andersen, K.H. Hole, K. V. Lund, K. Sundfør, G.B. Kristensen, H. Lyng, E. Malinen (2013) Pharmacokinetic parameters derived from dynamic contrast enhanced MRI of cervical cancers predict chemoradiotherapy outcome, Radiother. Oncol. 107: 117–122.
28. F. Kuang, Z. Yan, H. Li, H. Feng (2015) Diagnostic accuracy of diffusion-weighted MRI for differentiation of cervical cancer and benign cervical lesions at 3.0T: Comparison with routine MRI and dynamic contrast-enhanced MRI, J. Magn. Reson. Imaging. 42: 1094–1099.
29. H. Hawighorst, W. Weikel, P.G. Knapstein, M. V. Knopp, I. Zuna, S.O. Schönberg, P. Vaupel, G. van Kaick (1998) Angiogenic activity of cervical carcinoma: assessment by functional magnetic resonance imaging-based parameters and a histomorphological approach in correlation with disease outcome., Clin. Cancer Res. 4: 2305–2312.
30. V.N. Harry (2010) Novel imaging techniques as response biomarkers in cervical cancer, Gynecol. Oncol. 116: 253–261.
31. J.H. Kim, C.K. Kim, B.K. Park, S.Y. Park, S.J. Huh, B. Kim (2012) Dynamic contrast-enhanced 3-T MR imaging in cervical cancer before and after concurrent chemoradiotherapy, Eur. Radiol. 22: 2533–2539.
32. G. Christofori, H. Semb (1999) The role of the cell-adhesion molecule E-cadherin as a tumour-suppressor gene, Trends Biochem. Sci. 24: 73–76.
33. M. Herzig, F. Savarese, M. Novatchkova, H. Semb, G. Christofori (2007) Tumor progression induced by the loss of E-cadherin independent of β-catenin/Tcf-mediated Wnt signaling, Oncogene. 26: 2290–2298.
34. Choi SH, Kim SH, Choi HJ, Park BK, Lee HJ (2004) Preoperative magnetic resonance imaging staging of uterine cervical carcinoma: results of prospective study. J Comput Assist Tomogr 28:620–627.
35. Jena A, Oberoi R, Rawal S, Das SK, Pandey KK (2005) Parametrial invasion in carcinoma of cervix: role of MRI measured tumour volume. Br J Radiol 78:1075-1077.